

## **EFFECT OF GADOLINIUM(III) IONS ON THE PHASE BEHAVIOUR OF DIMYRISTOYLPHOSPHATIDYL SERINE MULTILAMELLAR LIPOSOMES**

*A. Averbakh<sup>1</sup>, D. Pavlov<sup>2</sup> and V. I. Lobyshev<sup>2\*</sup>*

<sup>1</sup>Institute of Chemical Physics in Chernogolovka, Moscow Region

<sup>2</sup>Physics Faculty, Moscow State University, 119899 Moscow, Russia

### **Abstract**

The effects of low concentrations of  $Gd^{3+}$  on dimyristoylphosphatidyl serine (DMPS) multilamellar liposomes were studied by differential scanning calorimetry (DSC). At low ionic strength merely a shifting upscale and a broadening of the main transition peak were observed. At high ionic strength,  $Gd^{3+}$  provoked the formation of a few clearly-discernible high-temperature components. Increase of the Gd level affected the relative intensities of these components, whereas the corresponding mid-points and half-widths remained unchanged. At the same time, in the presence of about 20 mol% dimyristoylphosphatidyl choline in the mixture with DMPS, similar secondary peaks appeared, but their positions were markedly shifted, to extents dependent on the Gd concentration. Interpretation of the data in terms of two-dimensional crystal structures is suggested.

**Keywords:** adsorption, differential scanning calorimetry, dimyristoylphosphatidyl serine, gadolinium(III), liposomes

### **Introduction**

Gadolinium and its hydrophilic complexes are finding increasing use as contrast-enhancing agents in clinical NMR imaging protocols [1]. In an effort to improve the design and interpretation of these protocols, there is a need to understand the interactions of such reagents with biological molecules and assemblies. Gadolinium ions effectively modify the activity of mechanosensitive and voltage-dependent channels (see, for example, [2, 3]).  $Gd^{3+}$  can directly induce conformational changes in some proteins [4], but the physiological effects of lanthanides are usually expected to result mainly from alterations in the membrane characteristics.

However, very little is known about the interactions of  $Gd^{3+}$  with biological membranes, and in particular those containing negatively charged lipid species.

Phosphatidylserine (PS) is the predominant anionic phospholipid in most mammalian cell membranes [5]. The midpoint of the gel to liquid-crystal state transition of PS liposomes is very sensitive to the physical state of the bilayers, changing even

\* Author for correspondence: E-mail: lob@school.phys.msu.su; Fax: (095)4454634

in response to sonication of a suspension [6]. The effects of low levels of polyvalent cations on DSC tracings of PS membranes usually appear simply as a broadening and shifting of the phase transition midpoint to higher temperatures [7–9]. For dilute suspensions of liposomes from neutral and acidic phospholipids, the main peak of the gel to liquid-crystal transition is usually split into two or more distinguishable components [6, 10, 11]. Identification of the structures, however, is highly complicated because the midpoints of the secondary transitions are gradually shifted upscale as the polyvalent cation concentration increase. In the present paper, we report the unusual observation of the midpoints and half-widths of the newly-formed components in the DSC curves of dimyristoylphosphatidyl serine (DMPS) remaining constant at various concentrations of Gd. A hypothesis is presented which ascribes the observed components to particular molecular structures.

## Materials and methods

The  $\text{GdCl}_3$  (Sigma Chemical Co., St. Louis, MO, USA) had a purity of 99.9%.  $\text{KCl}$  and  $\text{BeCl}_2$  were salts of reagent grade (Reachim, USSR). Imidazole (Calbiochem, Germany) was used to prepare buffer solutions. DMPS and dimyristoylphosphatidyl choline (DMPC) were purchased from Avanti Polar Lipids, Inc. (Birmingham, AL, USA). No detectable impurities were evident in either of these phospholipids on TLC. Their purity was further confirmed via the main transition peaks of their DSC curves [12, 13].

Multilamellar liposomes were prepared by evaporation for 2 h of a chloroform solution of the lipid in a 10 ml conical flask under vacuum and by gentle shaking of the flask (containing the thin lipid film) in the respective electrolyte. The polyvalent cation level was increased by successive additions of concentrated solutions (5–20  $\mu\text{l}$  aliquots) into suspensions of multilamellar liposomes at 18–20°C.

The calorimetric curves were obtained with a DASM-4 scanning micro-calorimeter (NPO Biopribor, Russia). Each sample had a volume of 0.47 ml, and an equal amount of buffer was placed in the reference cell. All scans were performed at a heating rate of  $1^\circ\text{C min}^{-1}$ , with a DMPS concentration of  $0.4 \text{ mg ml}^{-1}$  in all samples. In some cases, equilibration of the samples was carried out by heating up to 100 and then cooling down to 4°C (four cycles). All experiments were performed at least in duplicate to be certain that subtle effects were reproducible. Data are presented for representative experiments. Multiple peaks were resolved by using software provided by Microcal Origin, and individual peak areas were obtained with the same software. The least restrictive model of a deconvolution algorithm (independent, non-two-state transitions) was used. The model is based on the Levenberg/Marquardt non-linear least-square method. Finally, relative areas (relative integrated intensities) of the components were obtained by dividing the area of each component by the total area under the curve.

The light microscopic images of the DMPS suspensions were obtained with a Carl Zeiss Axioplan photomicroscope with a water immersion Plan-Neofluar 40 $\times$  objective. The video camera was a Quantix CCD camera KAF 1400-G1 with pixel size

6.8×6.8 μm (Photometrics Ltd., AZ, USA). The Petri dishes containing lipid suspensions were thermostated with a Red Beam incubator (Opti-Quip, Inc., New York). The digitized images were acquired by using Volume Scan IP software (Vay Tek Inc., USA).

## Results

The effects of  $Gd^{3+}$  on the DMPS multilamellar liposomes at low ionic strength (10 mM KCl, pH 7.1) are illustrated by the DSC curves in Fig. 1. The suspensions were fairly transparent and the gel to liquid-crystalline phase transition appeared to be described by one peak, which broadened and shifted to higher temperature as the total concentration of Gd was increased.

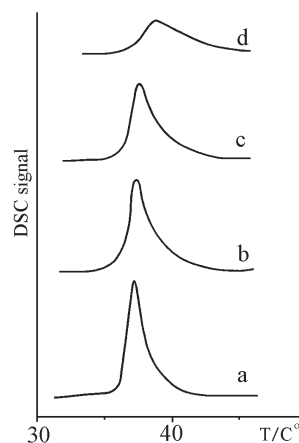


**Fig. 1** DSC heating curves of DMPS (0.4 mg ml<sup>-1</sup>) liposomes heated from 10°C at a rate of 1°C min<sup>-1</sup> in the presence of different total concentrations of Gd: a – 0.0 μM; b – 9 μM; c – 18 μM; d – 38 μM. Each sample comprised 0.47 ml aqueous suspension containing 10 mM KCl buffered to pH 7.1 with 2 mM imidazole and the indicated amount of GdCl<sub>3</sub>

At high ionic strength (500 mM KCl, pH 7.1), however, the samples were distinctly turbid and the presence of  $Gd^{3+}$  produced a much more complicated effect. At a total Gd concentration  $C_3=13$  μM, the enthalpy associated with the main peak was reduced, whereas the DSC curve broadened and two distinct shoulders were easily seen at higher temperatures (Fig. 2A (b)). When the Gd concentration was increased up to 27 μM, the main transition peak was further reduced and two high-temperature peaks appeared (Fig. 2A (c)). At Gd concentrations of 46 and then 64 μM, the newly formed component on the high-temperature edge of the DSC curve successively intensified, while the main transition peak gradually decreased (Fig. 2B (a, b)). Further, several shoulders protruded between the main transition peak and the high-temperature peaks. It is noteworthy that the two high-temperature peaks did not shift as the total concentration of Gd was increased, and they became centred at  $42.7\pm 0.2$  and

45.4±0°C (Fig. 2A and B). No indications of lipid precipitation were observed in this range of Gd concentrations, while the suspensions completely collapsed at  $C_3=200\ \mu\text{M}$ , with the formation of a grey film that covered the walls of the flask.

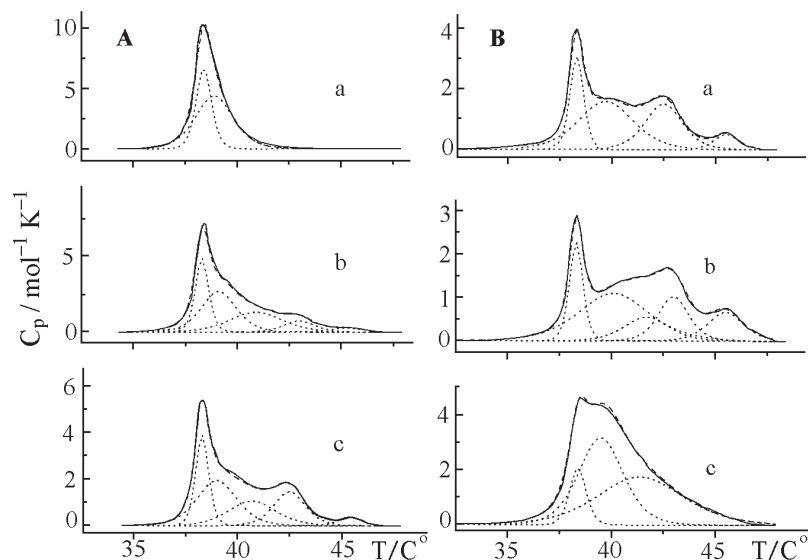


**Fig. 2** DSC heating curves of DMPS ( $0.4\ \text{mg ml}^{-1}$ ) liposomes heated from  $10^\circ\text{C}$  at a rate of  $1^\circ\text{C min}^{-1}$  in the presence of different total concentrations of Gd: (A): a –  $0.0\ \mu\text{M}$ ; b –  $13\ \mu\text{M}$ ; c –  $27\ \mu\text{M}$ ; (B): a –  $46\ \mu\text{M}$ ; b –  $64\ \mu\text{M}$ ; c –  $13\ \mu\text{M}$  (in case (c); the sample was preliminarily equilibrated via 4 heating and cooling cycles). Each sample comprised  $0.47\ \text{ml}$  aqueous suspension containing  $500\ \text{mM}$  KCl buffered to pH 7.1 with  $2\ \text{mM}$  imidazole. Deconvolution of the entire endotherms was performed as described in the ‘Materials and Methods’

In the case of a  $100\ \text{mM}$  KCl background electrolyte (pH 7.1), similar high-temperature components were also present, though less pronounced (data not shown). It should be noted that multiple secondary peaks appeared in the curves of DMPC multilamellar liposomes even at  $10\ \text{mM}$  KCl electrolyte (pH 7.1), but at much higher concentrations of Gd. In the latter case, the additional high-temperature peaks were clearly shifted upscale as the Gd concentration was increased (data not shown). Surprisingly, only one additional high-temperature component was present in the DSC curves of dipalmitoylphosphatidyl choline (DPPC) multilamellar liposomes [14], but its position was also shifted upscale on increase of the GD concentration.

The results of deconvolution analysis of the curves in Figs 2A and B are listed in Table 1. The original endotherm corresponding to pure DMPS in  $500\ \text{mM}$  KCl solution is satisfactorily described by two Gaussians centred at  $38.4$  and  $38.9^\circ\text{C}$ , with respective half-widths of  $0.9$  and  $2.1^\circ\text{C}$ . Two very similar components were found to contribute to the DSC curves at total Gd contents of  $13$  and  $27\ \mu\text{M}$  (Fig. 2A(b)

**Table 1** Thermodynamic characteristics of DMPS multilamellar liposomes melting in the presence and absence of Gd<sup>3+</sup> at high ionic strength (500 mM KCl, pH 7.1)

<i>C</i> <sub>3</sub> / μM	Deconvolution analysis															Total <i>H</i> / %
	peak 1			peak 2			peak 3			peak 4			peak 5			
	<i>T</i> <sub>m</sub>	Δ <i>T</i>	<i>H</i>	<i>T</i> <sub>m</sub>	Δ <i>T</i>	<i>H</i>	<i>T</i> <sub>m</sub>	Δ <i>T</i>	<i>H</i>	<i>T</i> <sub>m</sub>	Δ <i>T</i>	<i>H</i>	<i>T</i> <sub>m</sub>	Δ <i>T</i>	<i>H</i>	
0	38.4	0.9	40	38.9	2.1	60										339
13	38.3	0.7	24	39.1	1.9	37	40.9	2.9	28	43.0	1.7	9	45.3	1.6	2	337
27	38.3	0.7	22	39.0	2.2	33	40.7	2.6	21	42.5	1.8	21	45.4	1.5	3	301
46	38.3	0.8	20	39.7	3.1	43				42.5	2.0	29	45.5	1.4	8	266
64	38.3	0.7	17	40.1	3.9	40	41.7	2.5	13	43.0	1.7	17	45.5	1.9	13	238
13*	38.4	0.9		39.5	2.5	44	41.4	4.8	46							379

*T*<sub>m</sub>(°C), Δ*T* (°C) and *H* (%) are the transition midpoints, half-widths and relative integrated intensities, respectively

\* The indicated sample was equilibrated via 4 heating and cooling cycles

and (c)). These two components are likely to represent the gel to liquid-crystalline phase transition of the membranes, which do not contact the  $Gd^{3+}$ . Since the interactions of DMPS liposomes and  $Gd^{3+}$  at low concentrations do not cause significant changes in the overall area under the curves, the mole fraction of the lipid molecules which relates to the bilayers inaccessible to  $Gd^{3+}$  (trapped) may be roughly estimated as 55–63% (see data for the  $C_3=13$  and  $27 \mu M$  curves (Table 1)). These estimates are supported by DSC tracings illustrating the effects of low levels of  $Be^{2+}$  [11] on the DSC curves of DMPS multilamellar liposomes (Fig. 3) prepared in exactly the same way and with the same background electrolyte (500 mM KCl, pH 7.1). It is readily seen (Fig. 3) that the area corresponding to the inaccessible (to  $Be^{2+}$ ) membranes constitutes nearly 50–60% of the total area under the curve.

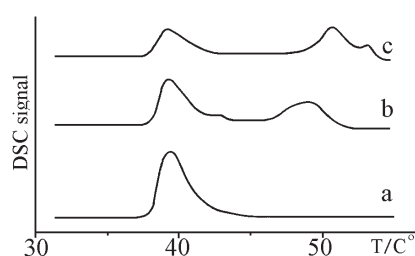


**Fig. 3** DSC heating curves of DMPS ( $0.4 \text{ mg ml}^{-1}$ ) liposomes heated from  $10^\circ\text{C}$  at a rate of  $1^\circ\text{C min}^{-1}$  in the presence of different total concentrations of Be: a –  $0.00 \text{ mM}$ ; b –  $0.06 \text{ mM}$ ; c –  $0.14 \text{ mM}$ . Each sample comprised  $0.47 \text{ ml}$  aqueous suspension containing  $500 \text{ mM}$  KCl buffered to pH 7.1 with  $2 \text{ mM}$  imidazole

At higher Gd concentrations, the left component of the main transition (centred at  $38.3^\circ\text{C}$ ) is still observed, whereas the other one (centred at about  $39.0^\circ\text{C}$ ) cannot be resolved from the middle component with the software available (Fig. 2B(a) and (b)). Deconvolution analysis of the DSC tracings obtained for the DMPS liposomes in the presence of Gd demonstrated that all the DSC curves contained two high-temperature components with essentially permanent positions centred at  $42.7 \pm 0.2$  and  $45.4 \pm 0.1^\circ\text{C}$  (Table 1). Moreover, they had nearly constant half-widths of  $1.8 \pm 0.1$  and  $1.6 \pm 0.2^\circ\text{C}$ , respectively. When the Gd concentration was increased up to  $46 \mu\text{M}$ , the relative integrated intensity of the endotherm centred at  $42.7^\circ\text{C}$  rose to its maximum value, and then diminished at  $C_3=64 \mu\text{M}$ . At the same time, the enthalpy associated with the component centred at  $45.4^\circ\text{C}$  monotonously increased with the Gd concentration (Table 1). The middle endotherms observed as one or two broad Gaussians with half-widths of  $1.9$ – $3.9^\circ\text{C}$  (corresponding to the shoulders in the DSC curves) could not be resolved into the individual components, and they may reflect the coexistence of several components with quite similar thermodynamic properties.

In general, the picture suggests the coexistence of several discrete Gd-containing lipid phases, whose molecular structures do not depend on the Gd concentration in the suspension. Further addition of Gd results only in the redistribution of the relative intensities of the coexisting components, during which the contributions from the

phases with higher contents of adsorbed  $\text{Gd}^{3+}$  (very probably the components appearing at higher temperatures) increase continuously.

Figure 2B(c) demonstrates that sample equilibration (multiple heating and cooling cycles) leads to a strong reduction of the component centred at  $38.3^\circ\text{C}$ , accompanied by the complete disappearance of the additional high-temperature peaks. From this fact, we may assume that these high-temperature components originate from the asymmetric distribution of polyvalent cation across the membranes [7, 15–17]. The DSC curves of the multilamellar liposomes containing ~20 mol% DMPC (a mixture of 0.4 DMPS and 0.1 mg  $\text{ml}^{-1}$  of DMPC in 500 mM KCl solution, pH 7.1) also indicated the presence of the very similar secondary high-temperature peaks (data not shown). In this case, however, the midpoints of the transitions were not constant and shifted markedly downscale as the Gd concentration was increased. This implies that even fairly small changes in the membrane surface charge density are important, and electrostatic forces may contribute considerably to the stability of the presumed  $\text{Gd}^{3+}$ -induced structures.

## Discussion

Light microscopic observation of the samples at 500 mM KCl revealed that the suspensions consist of liposomes with a wide size distribution ranging from 0.1 about  $15\ \mu\text{m}$ , in accordance with previously reported data [7, 17]. In general, at 500 mM KCl the diameter of the liposomes is on average 2–3 times larger than that at 10 mM background electrolyte (Fig. 4(a, b)) [13]. At 500 mM KCl, most of the particles are multilamellar liposomes with concentrically arranged bilayers, whereas the internal aqueous cavities often contain smaller vesicles at both high and low levels of background electrolyte [17, 18]. The addition of low levels of  $\text{GdCl}_3$  to the preformed suspensions leads to partial aggregation of the liposomes, but does not seem to result in their rupture or other visible deformation of the morphology (Fig. 4(c, d)). Inspection of hundreds of fields for ten different preparations at  $C_3=27$  and  $46\ \mu\text{M}$  Gd at  $20^\circ\text{C}$  did not reveal the presence of any repeating liposome assemblies with a regular arrangement, or any other regular supramolecular lipid structures. No discreteness in the size distribution of the liposomes in the presence of Gd was detected. Observation of the samples at  $45^\circ\text{C}$  did not indicate any significant morphological differences relative to those examined at  $20^\circ\text{C}$  (data not shown).

Some of the liposomes adhere and flatten against each other, forming tight contacts (Fig. 4(c–f)). The total area of the tight contacts progressively increases with increasing Gd concentration, but the arrangements of several internal lamellae stacked in an onion-like fashion [17] are conserved at these moderate Gd concentrations. This is in agreement with the DSC data, where the original component centred at  $38.3^\circ\text{C}$  remains significant at all studied Gd levels (Fig. 2). At the same time, the enthalpy for this endotherm gradually diminishes with increasing concentrations of  $\text{Gd}^{3+}$  and  $\text{Be}^{2+}$ , indicating partial penetration of the cations into the liposome interior (probably for separate liposome populations) [19]. In contrast, the contribution from this endotherm was strongly decreased after sample equilibration, even at a Gd level as low as  $13\ \mu\text{M}$  (Fig. 2B (c)).

The addition of polyvalent cations to suspensions of liposomes from negatively charged lipids usually leads to their sticking together and to the formation of aggregates of various sizes. A considerable agglomeration of DMPS liposomes also occurs after the addition of micromolar levels of  $\text{Li}^+$ ,  $\text{Ca}^{2+}$  [6, 12, 20] and  $\text{Be}^{2+}$  (Fig. 4(f)), but it does not result in the appearance of multiple secondary components with constant thermal characteristics. The aggregation of DMPS liposomes in the presence of micromolar concentrations of Be, Ca and Gd at low ionic strength (10 mM KCl, pH 7.1) is even more significant (see, for example, Fig. 4(e)). We argue, therefore, that the aggregation of liposomes itself cannot be the cause of the phenomenon. The aggregation of DMPS liposomes in the presence of micromolar concentrations of Be, Ca and Gd at low ionic strength (10 mM KCl, pH 7.1) is even more significant (see, for example, Fig. 4(e)). We argue, therefore, that the aggregation of liposomes itself cannot be the cause of the phenomenon. The slow penetration of  $\text{Gd}^{3+}$  across the concentric bilayers (experiencing different effective concentrations of Gd) also seems unlikely to result in the coexistence of stable discrete phases whose transition midpoints do not change. Thus, we hypothesize that adsorbed  $\text{Gd}^{3+}$  generates the formation of new two-dimensional crystal structures in DMPS bilayers, and the observed discrete components originate from discrete values of the surface concentration of bound  $\text{Gd}^{3+}$ . In other words, the presumed phases are determined by definite numbers  $N$  of lipid molecules within an accessible monolayer corresponding to one bound  $\text{Gd}^{3+}$  [8, 21]. Nothing is implied as to whether these different regular structures are located in different liposomes or are laterally separated within the continuous bilayers, or the nature of the boundaries between them.

A hint at the related regular structures is presented in [14], where freeze-fracture electron micrographs of DPPC liposomes demonstrate regular ripple patterns on the

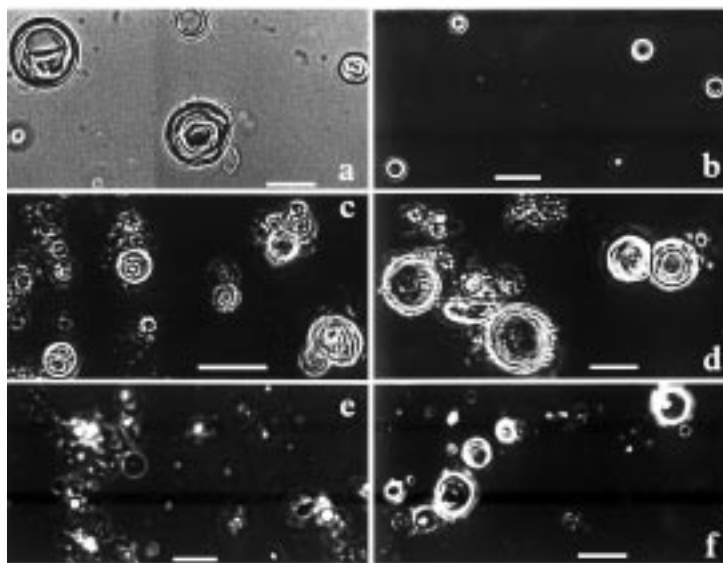


**Fig. 4** Light microscopical images of multilamellar DMPS ( $0.4 \text{ mg ml}^{-1}$ ) liposomes in aqueous (pH 7.1) suspensions containing: a – 500 mM KCl; b – 10 mM KCl; c – 500 mM KCl,  $27 \mu\text{M Gd}^{3+}$ ; d – 500 mM KCl,  $46 \mu\text{M Gd}^{3+}$ ; e – 10 mM KCl,  $38 \mu\text{M Gd}^{3+}$ ; f – 500 mM KCl,  $60 \mu\text{M Be}^{2+}$ . The bar represents 10  $\mu\text{m}$



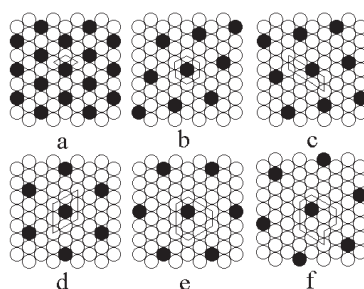


**Fig. 5** Examples of two-dimensional crystal phases with definite numbers  $N$  of lipid molecules within an accessible monolayer corresponding to one bound  $Gd^{3+}$

fracture face. The authors assumed that ‘these regular patterns are related in some way to the crystal packing of the phospholipid molecules’. Importantly, after the addition of  $La^{3+}$ , regular ripple patterns are likewise present, but certainly of a different kind [14]. No regular patterns are seen on freeze-fracture electron micrographs of brain PS liposomes in the absence or presence of  $Mg^{2+}$  and  $Ca^{2+}$  [7] or for mixtures of DPPC with brain PS [9]. At the same time, similar ripple patterns are found for a stable higher-melting gel phase of synthetic acidic lipid DMPG [22]. It has been shown that the transition to the new gel phase is initiated by changes in the interfacial and/or headgroup region of the bilayer. We suggest that the formation of multiple secondary phases of DMPS with constant thermodynamic characteristics might also originate from the regular binding of  $Gd^{3+}$  to the lipid headgroups, which can be different for various  $N$  values. Several examples of two-dimensional crystal phases are presented in Fig. 5, with  $N$  varying from 3 to 12. In the regions of tight contacts between the negatively charged liposomes, the binding affinity for polyvalent cations is much higher than for similar, isolated surfaces [23, 24], and both inter- and intra-bilayer binding is possible. The  $N$  value in these areas may therefore be significantly lower and determine different thermotropic properties. The surfaces with high  $N$  values probably correspond to small changes in transition midpoints and will not be resolved in the calorimetric curves constituting broad middle components. Moreover, the resolution becomes much weaker at 100 mM KCl, and completely disappears at 10 mM KCl, which might be related in some way to the sufficient decrease in liposome size.

\* \* \*

We are grateful to Dr. Yu. A. Ermakov for the kind gift of DMPS and DMPC preparations, and for critical comments.

## References

- 1 P. T. Normann and P. A. Hals, *Eur. J. Drug Met. Pharm.*, 20 (1995) 307.
- 2 C. Cui, D. O. Smith and J. Adler, *J. Membrane Biol.*, 144 (1995) 31.

- 3 B. Klusener, G. Boheim, H. Liß, J. Engelberth and E. W. Weiler, *EMBO J.*, 14 (1995) 2708.
- 4 C. Soto, P. H. Rodriguez and O. Monasterio, *Biochemistry*, 35 (1996) 6337.
- 5 G. Rouser, G. J. Nelson, S. Fleischer and G. Simon, *Biol. Membr.*, 1 (1968) 5.
- 6 H. Hauser and G. G. Shipley, *Biochemistry*, 23 (1984) 34.
- 7 D. Papahadjopoulos, W. J. Vail, C. Newton, S. Nir, K. Jacobson, G. Poste and R. Lazo, *Biochim. Biophys. Acta*, 465 (1977) 579.
- 8 C. Newton, W. Pangborn, S. Nir and D. Papahadjopoulos, *Biochim. Biophys. Acta*, 506 (1978) 281.
- 9 S. W. Hui, L. T. Boni, T. P. Stewart and T. Isac, *Biochemistry*, 22 (1983) 3511.
- 10 M. G. Ganesan, D. L. Schwinke and N. Weiner, *Biochim. Biophys. Acta*, 686 (1982) 245.
- 11 Yu. A. Ermakov, S. S. Mahmudova, E. V. Shevchenko and V. I. Lobyshev, *Biol. Membr.*, 10 (1993) 212.
- 12 H. Hauser and G. G. Shipley, *J. Biol. Chem.*, 256 (1981) 11377.
- 13 R. M. Epand and S. W. Hui, *FEBS Lett.*, 209 (1986) 257.
- 14 Xin-min Li, Ya-fei Zhang, Jia-zuan Ni, Jian-wen Chen and Fen Hwang, *J. Inorganic Biochem.*, 53 (1994) 139.
- 15 M. A. Akeson, D. N. Munns and R. G. Burau, *Biochim. Biophys. Acta*, 986 (1989) 33.
- 16 R. Lehmann and J. Seelig, *Biochim. Biophys. Acta*, 1189 (1994) 89.
- 17 H. Hauser, *Biochim. Biophys. Acta*, 772 (1984) 37.
- 18 B. Kachar, N. Fuller and R. P. Rand, *Biophys. J.*, 50 (1986) 779.
- 19 S. J. Rehfeld, L. D. Hansen, E. A. Lewis and D. J. Eatough, *Biochim. Biophys. Acta*, 691 (1982) 1.
- 20 S. McLaughlin, N. Mulrine, Th. Gresalphi, G. Vaio and A. McLaughlin, *J. Gen. Physiol.*, 77 (1981) 445.
- 21 L. J. Lis, V. A. Parsegian and R. P. Rand, *Biochemistry*, 20 (1981) 1761.
- 22 R. M. Epand, B. Gabel, R. F. Epand, A. Sen, S. W. Hui, A. Muga and W. K. Surewicz, *Biophys. J.*, 63 (1992) 327.
- 23 R. P. Rand and V. A. Parsegian, *Can. J. Biochem. Cell. Biol.*, 62 (1984) 752.
- 24 J. R. Coorsen and R. P. Rand, *Biophys. J.*, 68 (1995) 1009.